

Direct micro-patterning of biodegradable polymers using ultraviolet and femtosecond lasers

Carlos A. Aguilar^a, Yi Lu^a, Samuel Mao^b, Shaochen Chen^{a,*}

^aDepartment of Mechanical Engineering, University of Texas at Austin, Austin, TX 78712, USA

^bDepartment of Mechanical Engineering, University of California at Berkeley, Berkeley, CA 94720, USA

Received 18 November 2004; accepted 20 April 2005

Available online 13 June 2005

Abstract

Thin films of biodegradable polymeric materials, poly(ϵ -caprolactone) (PCL) and poly(glycolic acid) (PGA) were micro-patterned using a Ti-sapphire femtosecond pulsed laser and ArF excimer UV laser in ambient conditions. The laser-patterned polymers were characterized using a scanning electron microscope (SEM), Fourier transform infrared spectroscopy in attenuated total reflectance mode (FTIR-ATR) and X-ray photoelectron spectroscopy (XPS). In-vitro degradation tests were performed and the laser-patterned samples showed to be within one standard deviation of the control samples. Our results demonstrate that both lasers are excellent tools for micro-patterning biodegradable polymers since the bulk properties of the material can remain intact and because the direct-write method is rapid, flexible, and a chemical-free process.

© 2005 Elsevier Ltd. All rights reserved.

Keywords: Biodegradable polymer; Laser micromachining; Femtosecond laser; Excimer laser; Photothermal; Photochemical; Hydrolytic degradation

1. Introduction

Biodegradable polymeric materials have had a significant impact on medical technology, greatly enhancing the efficacy of many existing drugs and enabling the construction of entirely new therapeutic modalities [1]. These degradable elastomers have been employed in many areas of therapeutic medicine from commonly used resorbable surgical sutures [2], to next-generation controlled-release drug delivery vehicles [3] and implantable cell-support scaffolds [4,5]. Of the many biodegradable synthetic polymers, the aliphatic polyesters have gained considerable interest because of their unique ability to hydrolytically degrade through ester linkage via metabolic pathways [6]. The aliphatic polyesters poly(glycolic acid) (PGA) and poly(ϵ -caprolactone) (PCL) have both been approved by the Food and Drug Administration for human clinical use in vivo

[7]. PGA is the simplest linear aliphatic polyester and was developed as the first totally synthetic absorbable suture [8,9]. It is highly crystalline with a high melting point and a low solubility in most common organic solvents [10]. PCL is a semi-crystalline polyester with a low tensile strength when compared to PGA, but it does exhibit a very high ultimate elongation. It is regarded as a soft and hard-tissue compatible material that is highly hydrophobic and has been used recently for bone graft substitutes [11,12]. A variety of factors such as process conditions and monomer selection will affect the material properties including crystallinity, melt and glass-transition temperatures, molecular weight, and end groups of the polymer, which in turn influence the degradation rate [13,14].

The development of next generation drug delivery and tissue engineering devices based on biodegradable polymers are contingent on the fashioning of features analogous to the size of cells and organelles [15]. Currently, the techniques for generating micro- and nano-patterns on polymeric materials include soft

*Corresponding author. Tel.: +1 512 232 6094.

E-mail address: schen@mail.utexas.edu (S. Chen).

lithography, photolithography, and atomic force microscopy etching (AFM) [16,17]. Soft lithography techniques such as micro-contact printing allow rapid manufacturing at a low cost and it is expected that such fabrication techniques will not alter the integrity of the polymers. However, soft lithography is still restricted by the development of appropriate masters. Photolithography has been proven to be a powerful tool for patterning engineering materials with a high resolution. Yet, the process involves multiple steps that make use of chemical solvents and furthermore, the residual chemical agents left on the polymer surface after fabrication could be toxic if implanted, as most biodegradable polymers would be. AFM etching is a process used to create sub-micron features by scratching the surface of the material with a nano-sized pyramidal tip. The technique allows for high precision but it is hindered by the speed of processing and cannot be used efficiently to etch large surface areas. Therefore, a minimally invasive and rapid technique to pattern polymers on the micro- and nano-scale, where the integrity of the polymeric substrate can be maintained after processing is needed.

Laser micromachining has been proven an excellent technique for patterning many engineering materials [18]. The method is a single-step process that directly removes the material through solid-vapor ablation, minimizing the thermal damage to the surrounding material. Ultraviolet lasers can modify the surface of a material through direct chemical bond breaking [19]. The emitted photon energy from a UV laser is high enough to break the chemical bonds of the target material directly, thereby minimizing the heat effects to the surrounding material. This feature makes UV laser micromachining very attractive for biodegradable polymeric materials, since thermal damage to the non-processed area can be dramatically reduced. Another possible means of micromachining polymers with precise resolution is through the use of solid-state femtosecond lasers. This type of laser has gained interest recently because the influence of heat conduction around the machined area can typically be ignored. This can be accomplished primarily because of the short time scale of laser–material interaction and since the localization of the excitation energy is very confined. This aspect makes the use of femtosecond laser pulses very appealing for micropatterning biodegradable polymers [20,21].

In this work, we make use of pulsed-laser micromachining to generate high-resolution micropatterns on biodegradable polymers. Both the UV and Ti:Sapphire femtosecond lasers were utilized for patterning PCL and PGA. Parametric investigations and material analysis aim to reveal the chemical and physical mechanisms of surface patterning associated with laser processing. Finally, *in vitro* degradation tests

were carried out to study the laser effect on material properties.

2. Materials and methods

2.1. Materials

PGA ($M_w = >100,000$, $T_g = 36^\circ\text{C}$) pellets were used as received from Polysciences Inc. PCL ($M_w \approx 50,000$, $T_g = -60^\circ\text{C}$) powder was used as received from Birmingham Polymers. Thermo-compression-molded films of size ($3\text{ cm} \times 2\text{ cm}$) were obtained by compressing solid PCL between two flat, rigid, parallel plates at 140 kPa and 30°C for 10 min. Solid PGA was thermopressed at 140 kPa and 50°C for 10 min. The film thicknesses were measured using a surface profilometer to be approximately $400\ \mu\text{m}$ thick before laser patterning.

2.2. Laser micromachining setup

Two laser systems (ArF excimer laser and Ti:Sapphire femtosecond laser) were used to micropattern the samples. The ArF excimer laser (Lambda Physik) has wavelength of 193 nm, pulse duration of 35 ns, 0.1–2.0 mJ/pulse energy, and 2 kHz repetition rate. The regeneratively amplified Ti:Sapphire mode-locked femtosecond laser system has 800 nm wavelength, 220 fs pulse duration, 0.1–1 μJ /pulse energy, and 1 kHz repetition rate. Fig. 1 shows a schematic diagram of the laser micromachining setup. The laser beam passes through a rectangular aperture where it is cropped in size to 8 mm and then through a beam splitter to reduce the energy. The cropped laser beam was then focused down through an objective lens for micropatterning of polymers.

2.3. Material characterization

Scanning Electron Microscopy (SEM) (LEO 1530) was used to observe the structures on the surface of the polymeric materials patterned by the laser direct-write method. A surface profilometer (Tencor Alpha Step 500) was used to scan across the etched areas to determine the ablation depth and cross-sectional profile. Fourier Transform Infra-Red Spectroscopy (MATTSON Spectrometer) in Attenuated Total Reflection mode (FTIR-ATR) was used to assess the bulk chemical

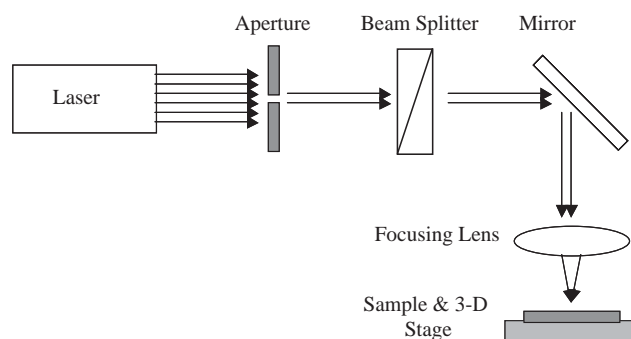


Fig. 1. Schematic setup of laser micromachining.

change of the laser processed samples. The FTIR-ATR has a 400–4000 cm^{-1} optical range with a 4 cm^{-1} resolution. The surface composition of the polymer layers was analyzed by X-ray photoelectron spectroscopy (XPS). The spectra was taken on a PHI 5700 XPS system using a monochromatic Al X-ray source operated at pass energies of 117.4 eV for surveys and 11.7 eV for high-resolution scans. The take-off angle of photoelectrons was 45° and the binding energy was calibrated using Au4f, Cu2p and Ag3d.

2.4. In-vitro degradation

Gravimetric weight loss of each sample was monitored weekly after maintaining the samples at 37°C in phosphate-buffer saline (PBS; pH 7.4). The buffer solution was changed once a week. Before each sample was weighed, it was washed in deionized water and immersed into liquid nitrogen for 30 s. The samples were then placed into a lypholizer (LABCONCO Freeze Dry System 4.5) for approximately 6 h and then weighed in ambient conditions. Degradation was calculated as a percentage weight loss according to the following equation:

$$\text{Percentage weight loss (\%)} = (W_i - W_t) / W_i \times 100, \quad (1)$$

where W_i is the initial dry weight of the sample and W_t is the dry weight of the sample following degradation at various time points. The results reported are an average of four measurements \pm standard deviation. To determine the maximum effect for laser processing effects on the degradation characteristics of the polymers, the entire surface of the thin film was patterned and tested against thin films of the same size and morphology for differences in degradation rates.

3. Results and discussion

As can be seen in Fig. 2, a thin film of PCL was successfully micromachined with the UV laser ($\lambda = 193 \text{ nm}$). It was reported that when a pulsed UV laser irradiates the surface of an organic polymer, depending upon the incident wavelength, pulse number and laser intensity, a range of several hundred nanometers to several microns of the surface of the material could be etched away with a geometry that is defined by the incident light beam. The ablation is then accompanied by an ejection of particulate matter and gases (CO_2 , C_2 and CO) and an audible shockwave can be heard because of the interaction of an intense laser pulse with the polymeric material [22]. After the first pulse was deposited, the etch depth was determined to follow a linear relationship with the successive pulses. In Fig. 3, the etch depth vs. pulse number curves are shown for PCL and PGA polymers. The slope of the lines in Fig. 3 give an approximate value for the etch depth/pulse for PGA (0.5 $\mu\text{m}/\text{pulse}$) and PCL (0.46 $\mu\text{m}/\text{pulse}$). The surface modifications performed by UV laser irradiation approximately followed Beer's Law [23]:

$$L_f = (1/\alpha) \ln(F/F_{\text{th}}), \quad (2)$$

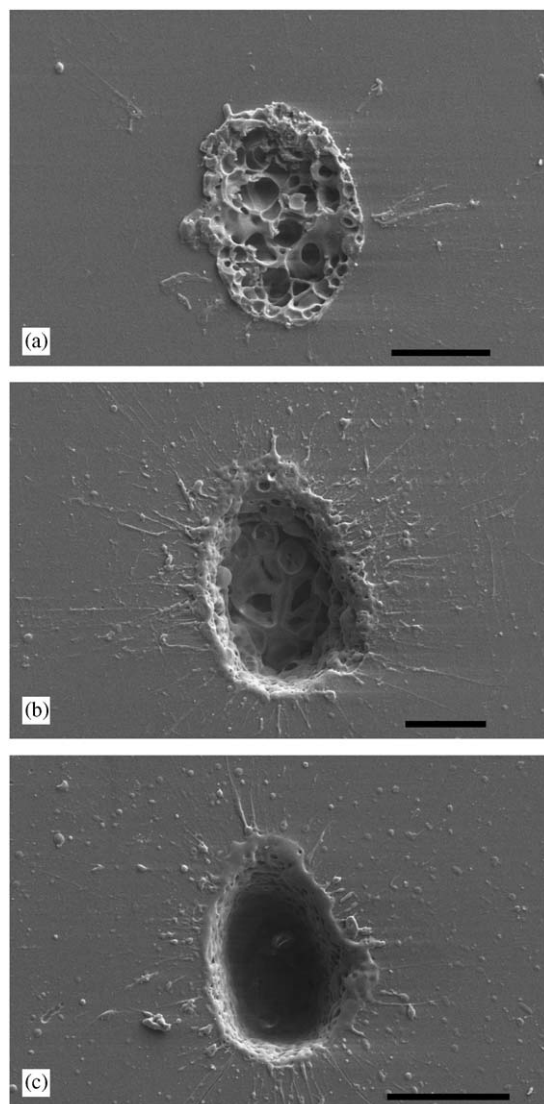


Fig. 2. SEM micrographs of PCL surface ablated with $\lambda = 193 \text{ nm}$ and pulse energy of 0.7 mJ/pulse. Scale bar is 30 μm . (a) Microhole etched with 1 pulse, (b) 10 pulses and (c) 20 pulses.

where L_f is the etch depth per pulse, α is the absorptivity of the material (cm^{-1}), F is the laser fluence and F_{th} is the threshold fluence of the material. The threshold fluence is the minimum intensity needed to initiate the ablation process and is specific for every material at different wavelengths. The threshold fluence of both polymers was measured by patterning the surface with various pulse energies with the same pulse number. The lowest energy deposited where ablation was seen was noted as the threshold fluence. To obtain the absorption coefficient, we first measured the etch depth per pulse by patterning holes and channels with the UV laser ($\lambda = 193 \text{ nm}$) with the same energy and various pulse numbers. We inspected the approximate depth of each pulse number deposited using a surface profilometer and

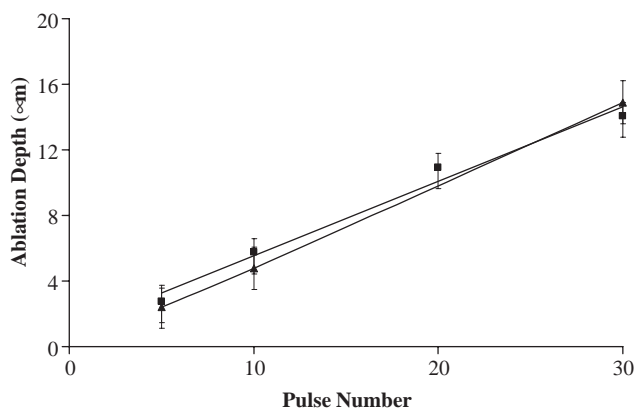


Fig. 3. Etch depth vs. pulse number using ArF excimer laser with $\lambda = 193$ nm for PCL ($\blacksquare = 0.33$ J/cm², pulse width = 35 ns) and PGA ($\blacktriangle = 0.4$ J/cm², pulse width = 35 ns).

determined an average value for the etch depth per pulse. Once the etch depth per pulse could be determined, we could then use Beer Lambert's law with known values of the laser fluence and threshold fluence to backcalculate the absorption coefficient. The threshold fluence and absorptivity were determined to be 0.4 J/cm² and 0.58×10^4 cm⁻¹ for PGA and 0.2 J/cm² and 1.1×10^4 cm⁻¹ for PCL, respectively. For laser fluences far above the threshold fluence, thermal effects such as melting begin to contribute to the etch depth. Additionally, it has been demonstrated that longer wavelengths pose stronger thermal effects on the material [24].

There have been various models including photochemical, photothermal or combination of photochemical and photothermal ablation mechanisms proposed to study the mechanism of UV laser ablation in polymers. For photochemical ablation to occur, energy of the emitted photons should be greater than the chemical bond energies of the material (Table 1). Since the incident photon energy is greater than the intermolecular bond energies of the polymer, the bonds are chemically broken through laser irradiation. The relation between the photon energy of light and laser wavelength is given by $E = 1.245/\lambda$, where λ is the laser wavelength and E is the photon energy. The photon energy decreases as the wavelength increases. In photothermal ablation, the material is first melted and eventually vaporized [25,26]. From Fig. 2, it can be argued that PCL experienced both a photochemical and photothermal effect because some melting and redeposition of the material along the edges was visible.

Previous research established the importance of multiple pulses in patterning a polymer with femtosecond lasers and determined that a single pulse did not produce a clear ablation edge but rather an inhomogeneous shape [27,28]. This effect can be seen in Figs. 4 and 5, where the surfaces patterned with multiple pulses

Table 1
Chemical bond energies for selected polymers

Polymer bonds	C–N	C–H	C=C	O–O	C=C	C–C	N–N	H–H
Bond energy (eV)	3.04	4.30	8.44	5.12	6.40	3.62	9.76	4.48

exhibited clean-cutting with little to no melting and very little debris along the edges. The surfaces patterned with a single pulse displayed rough edges with variations in etch depth. For both of the polymers patterned, the ablation depth increased with higher pulse numbers and the width of the holes and channels increased with stronger pulse energies. The irregularities in the hole shape were attributed to the noncircularity of the original laser beam. However, it should be noted that using advanced laser beam delivery systems, the irregularity of the hole shape can be corrected.

The ablation mechanisms associated with femtosecond laser pulses consist of the following two steps: First, the irradiated laser energy is absorbed inside the surface layer by bound and free electrons, which leads to excitation and ionization of the material. Second, the rapid absorption of laser energy is followed by energy transfer to the atomic sub-system. The overheated electrons transfer the energy to the lattice, which leads to bond breaking and material expansion. Thermal diffusion effects are considered negligible due to the short interaction time of the order of picoseconds. Therefore, the ablation occurs without the formation of burrs or heat-affected zones [15,29,30].

The changes in the chemical composition of the polyesters, before and after laser irradiation, were analyzed by FTIR-ATR and XPS. Figs. 6 and 7 show the IR spectra for PCL and PGA, respectively. In Fig. 6, the peaks in the characteristic bands at 2917 and 2851 cm⁻¹ correlate to both asymmetric and symmetric stretching of the CH₂ groups. The increase in the absorbance peaks around 1294 cm⁻¹ was assigned to the backbone C–C and C–O stretching modes in crystalline PCL [31]. The presence of this band at 1294 cm⁻¹ justifies the high crystallinity of the polymer [32]. As seen in Fig. 7, noticeable absorbance peaks at 3415 cm⁻¹ (O–H stretch) and at 2920/2850 cm⁻¹, which were attributed to the presence of C=H bonds, were observed. The existence of strong peaks at 1600 cm⁻¹, associated with the C=O in acetate end group and at 1425 cm⁻¹ (COO and CH–bend) was also seen. Figs. 8 and 9 show the XPS spectra for PGA. XPS helped us determine the elemental and average chemical composition of specific atoms of the material at its surface in 5–10 nm depths by measuring the binding energy of electrons associated with those atoms. The XPS spectra measured were the composition of carbon and oxygen atoms in each material. As can be seen in Table 2, the

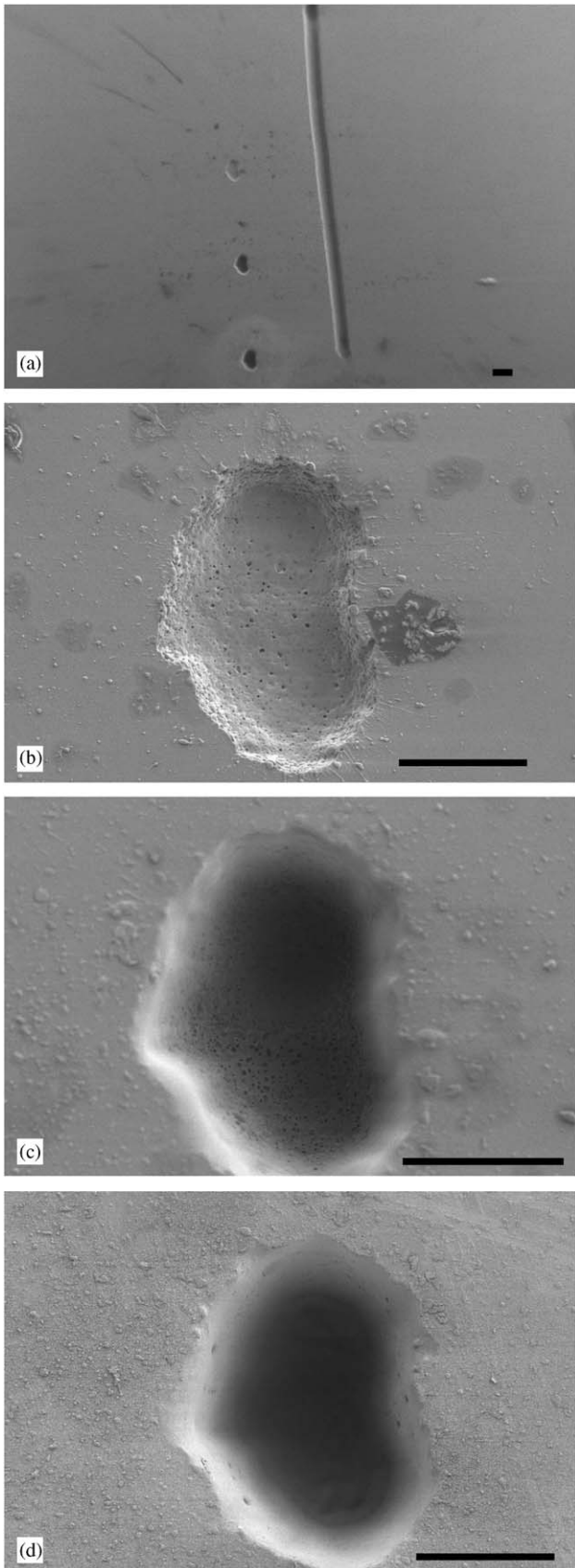


Fig. 4. SEM micrographs of PGA surface ablated with a pulse energy of $30\ \mu\text{J}/\text{pulse}$. Scale bar for (a) is $100\ \mu\text{m}$ and the scale for (b)–(d) is $30\ \mu\text{m}$. (a) Microfeatures etched in PGA, (b) microhole etched with 1 pulse, (c) 10 pulses and (d) 20 pulses.

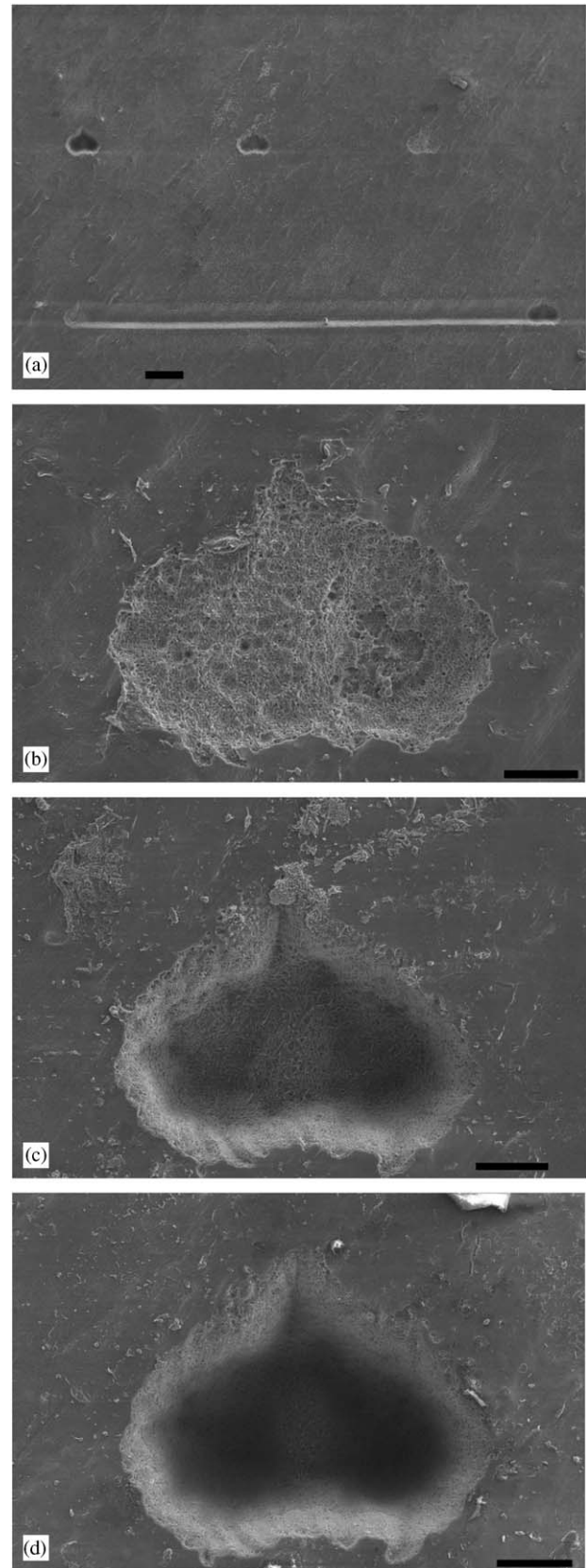


Fig. 5. SEM micrographs of PCL surface ablated with a pulse energy of $20\ \mu\text{J}/\text{pulse}$. Scale bar for (a) is $100\ \mu\text{m}$ and the scale for (b)–(d) is $20\ \mu\text{m}$. (a) Microfeatures etched in PCL, (b) Microhole etched with 1 pulse, (c) 10 pulses and (d) 20 pulses.

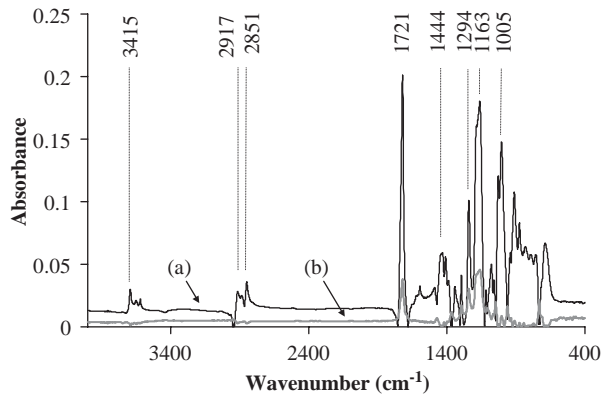


Fig. 6. FTIR-ATR spectra of PCL before (a) and after (b) laser irradiation with $\lambda = 193$ nm.

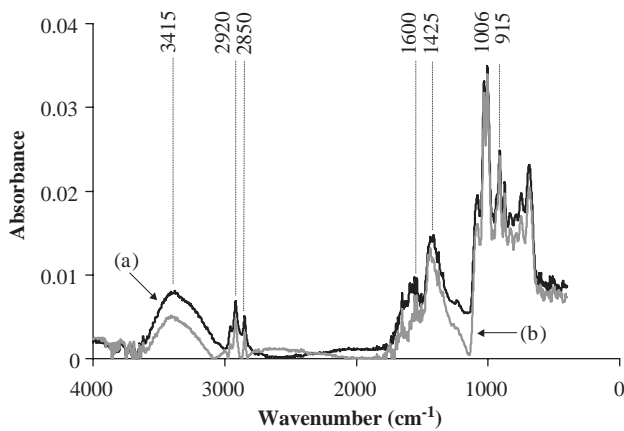


Fig. 7. FTIR-ATR spectra of PGA before (a) and after (b) laser irradiation with $\lambda = 193$ nm.

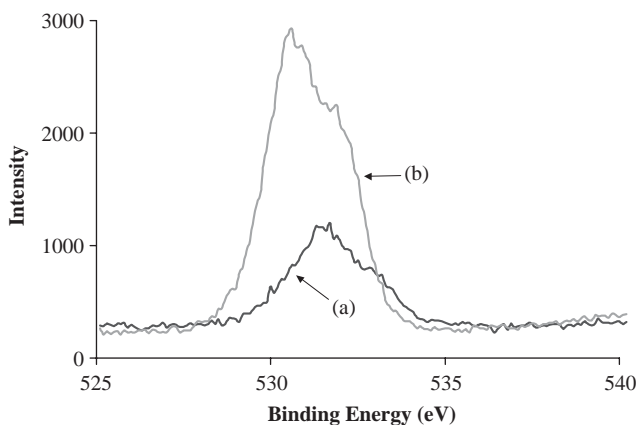


Fig. 8. XPS comparison of the O 1s region of PGA before (a) and after (b) laser irradiation with UV laser, $\lambda = 193$ nm.

laser irradiation induced a large decrease in the oxygen peak and a sizeable increase in the photoemission of carbon. The oxygen gain and decrease in carbon can be attributed to the loss of small gaseous molecules such as

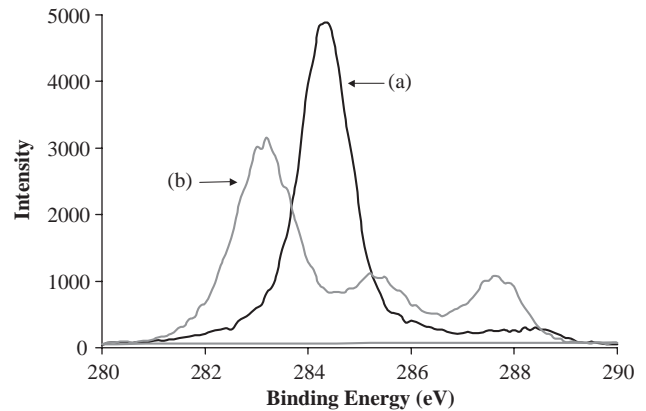


Fig. 9. XPS comparison of the C 1s region of PGA before (a) and after (b) laser irradiation with UV laser, $\lambda = 193$ nm.

Table 2

XPS comparison of the concentration of carbon and oxygen atoms before and after laser irradiation with UV laser ($\lambda = 193$ nm)

Polymer	Element	Concentration of original sample (%)	Concentration of laser treated sample (%)
PGA	C 1s	72.95	59.88
PGA	O 1s	27.05	40.12
PCL	C 1s	76.04	74.52
PCL	O 1s	23.96	25.48

CO_2 and CO , where both chemical and thermal decomposition of polymers are known to yield such products [33].

It was demonstrated that the aliphatic polyesters PCL and PGA undergo a two-step process for hydrolytic degradation [34]. The first step in the biodegradation process was a decrease in the molecular weight produced by random hydrolytic ester cleavage, and its duration is influenced greatly by the initial molecular weight as well as its chemical structure [35]. The second stage was distinguished by an onset of weight loss and a change in the rate of chain scission. As seen in Figs. 10 and 11, the laser processing had no significant effect on the degradation characteristics of the polymers. PCL experienced approximately a one percent weight loss over the 8-week test period and the difference between the laser treated sample and untreated sample were within one standard deviation of each other. PGA had approximately a 90% weight loss through the 8-week period and showed a disparity of one standard deviation between the laser processed sample and original sample.

4. Conclusions

We have utilized laser micromachining techniques for direct patterning biodegradable polymers for potential

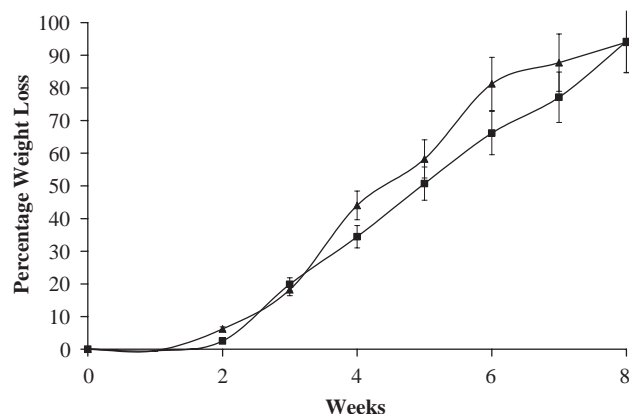


Fig. 10. In vitro degradation of PGA in PBS over 8 weeks. (■ = control sample, ▲ = laser treated sample with $\lambda = 193$ nm) Values reported are an average of four measurements \pm standard deviation.

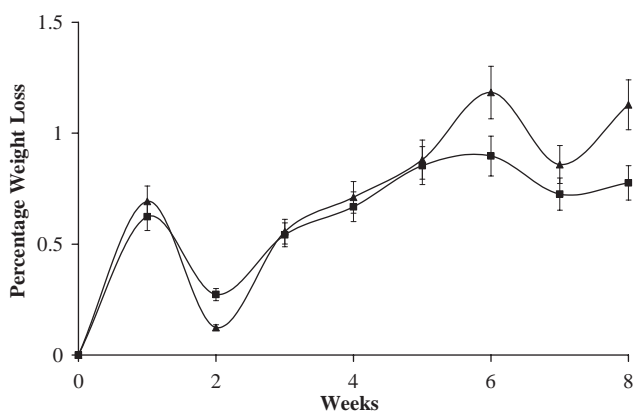


Fig. 11. In vitro degradation of PCL in PBS over 8 weeks. (■ = control sample, ▲ = laser treated sample with $\lambda = 193$ nm) Values reported are an average of four measurements \pm standard deviation.

applications in biomedical engineering. Micron-sized channels and holes were etched successfully in biodegradable polymers, which would be an integral part of many biodegradable microdevices. The effect of laser-polymer interaction on the chemical structure and degradation rate were studied and reported. It is concluded that both the femtosecond and UV lasers are excellent tools for micropatterning biodegradable polymers as a rapid, direct-write, flexible, and chemical-free process.

Acknowledgments

The project was supported by a CAREER award (DMI 0093364) to SC from the US National Science Foundation. The SEM analysis was conducted in the Texas Materials Institute at the University of Texas at Austin. The authors would like to thank Pavlos Tsiartas for his help and input with the excimer laser setup, Dr.

Krishnendu Roy for the use of his lab for the degradation tests, and Dr. Yangming Sun for his help with the XPS results.

References

- [1] LaVan DA, McGuire T, Langer R. Small-scale systems for in vivo drug delivery. *Nat Biotech* 2003;21(10):1184–91.
- [2] Behraves E, Yasko AW, Engle PS, Mikos AG. Synthetic biodegradable polymers for orthopaedic applications. *Clin Orthop* 1999;367(S):118–85.
- [3] Allen TM, Cullis PR. Drug delivery systems: entering the mainstream. *Science* 2004;303(5665):1818–22.
- [4] Duailibi SE, Duailibi MT, Pontes P, Young C, Vacanti JP, Yelick PC, Bartlett J. Tooth bioengineered on PGA & PLGA scaffolds in rat jaw. *J Dental Res* 2004;82(C):266.
- [5] Middleton JC, Tipton AJ. Synthetic biodegradable polymers as orthopaedic devices. *Biomaterials* 2000;21(23):2335–46.
- [6] Kancharla VV, Chen SC. Fabrication of biodegradable polymeric micro-devices using laser micromachining. *Biomed Microdevices* 2002;4(2):105–9.
- [7] Gunatillake PA, Adhikari R. Biodegradable synthetic polymers for tissue engineering. *Eur Cells Mater* 2003;5:1–16.
- [8] Kohn J, Langer R. Bioresorbable and bioerodible materials. In: Ratner BD, Hoffman AS, Schoen FJ, Lemons JE, editors. *Biomaterials science*. New York: Academic Press; 1996. p. 64–72.
- [9] Shalaby SW, Johnson R. Synthetic absorbable polyesters. In: Shalaby SW, editor. *Biomedical polymers designed to degrade systems*. New York: Hanser; 1994. p. 1–34.
- [10] Kyung-Bok L, Dong JK, Zee-Won L, Seong IW, Insung SC. Pattern generation of biological ligands on a biodegradable poly(glycolic acid) film. *Langmuir* 2004;20:2531–5.
- [11] Kweon H, Yoo M, Park IK, Kim TH, Lee HC, Lee HS, Oh JS, Akaike T, Cho CS. A novel degradable polycaprolactone networks for tissue engineering. *Biomaterials* 2003;24(5):801–8.
- [12] Piskin E. Biodegradable polymers in medicine. In: Scott G, editor. *Degradable polymers: principles and applications*. Netherlands: Kluwer; 2002. p. 321–79.
- [13] Kumar G. *Biodegradable polymers: prospects and progress*. New York: Marcel Dekker; 1987. p. 25–39.
- [14] Karsten M. Pharmaceutical applications of in-vivo EPR. *Phys Med Biol* 1998;43(7):1931–5.
- [15] Schmalenberg K, Uhrich K. Micropatterned polymer substrates control alignment of proliferating Schwann cells to direct neuronal regeneration. *Biomaterials* 2005;26:1423–30.
- [16] Xia Y, Whitesides GM. Soft lithography. *Ann Rev Mater Sci* 1998;28:153–84.
- [17] Boisen A, Hansen O, Bouwstra S. AFM probes with directly fabricated tips. *J Micromech Microeng* 1996;6:58–62.
- [18] Bauerle D. *Laser processing and chemistry*. Berlin: Springer-Verlag; 2000. p. 261–83.
- [19] Kokai F, Niino H, Yabe A. Rapid communication: laser ablation of polysulfone films: a laser ionization TOF mass spectrometric study. *Appl Phys A* 1998;67(5):607–12.
- [20] Baudach S, Bonse J, Kruger J, Kautek W. Ultrashort pulse laser ablation of polycarbonate and polymethylmethacrylate. *Appl Surf Sci* 2000;154–155:555–60.
- [21] Katayama S, Horiike M, Hirao K, Tsutsumi N. Structures induced by irradiation of femtosecond laser pulses in polymeric materials. *J Polym Sci B: Polym Phys* 2002;40:537–44.
- [22] Srinivasan R, Garrison BJ. Microscopic model for the ablative photodecomposition of polymers by far-ultraviolet radiation (193 nm). *Appl Phys Lett* 1984;44(9):849–51.
- [23] Srinivasan R. Ablation of polymers and biological tissue by ultraviolet lasers. *Science* 1986;234:559–65.

- [24] Chen SC, Kancharla V, Lu Y. Laser-based microscale patterning of biodegradable polymers for biomedical applications. *Int J Mat Products Tech* 2003;18(4):457–68.
- [25] Arnold N, Bityurin N, Bauerle D. Laser-induced thermal degradation and ablation of polymers: bulk model. *Appl Surf Sci* 1999;138:212–8.
- [26] Srinivasan V, Smith MA, Babu SV. Excimer laser etching of polymers. *J Appl Phys* 1990;59:3861–7.
- [27] Serafetinides AA, Skordoulis CD, Makropoulou MI, Kar AK. Picosecond and subpicosecond visible laser ablation of optically transparent polymers. *Appl Surf Sci* 1998;135:276–82.
- [28] Wang Z, Hong M, Lu Y, Wu D, Lan B, Chong T. Femtosecond laser ablation of polytetrafluoroethylene (Teflon) in ambient air. *J Appl Phys* 2003;93(10):6375–80.
- [29] Toenschhoff HK, Ostendorf A, Nolte S, Korte F, Bauer T. Micromachining using femtosecond lasers. *SPIE* 2000;4088: 136–9.
- [30] Von der Linde D, Sokolowski-Tinten K. The physical mechanisms of short-pulse laser ablation. *Appl Surf Sci* 2000;154:1–10.
- [31] Coleman M, Zarian J. FTIR studies of polymer blends: Poly(ϵ -caprolactone)-poly(vinyl chloride) system. *J Polym Sci B* 1979;17:837–50.
- [32] Elzein T, Nasser-Eddine M, Delaite C, Bistac S, Dumas P. FTIR study of polycaprolactone chain organization at interfaces. *J Coll Interface Sci* 2004;273:381–7.
- [33] Lazare S, Srinivasan R. Surface-properties of Poly(ethylene-terephthalate) films modified by far-ultraviolet radiation at 193-nm laser and 185-nm low intensity. *J Phys Chem* 1986;90(10):2124–31.
- [34] Cha Y, Pitt CG. The biodegradability of polyester blends. *Biomaterials* 1990;11:108–12.
- [35] Pitt CG, Gratzl MM, Kimmel GL, Surles J, Schindler A. Aliphatic polyesters II, the degradation of poly(D,L-lactide), poly(ϵ -caprolactone), and their copolymers in vivo. *Biomaterials* 1981;2:215–20.